Available online at www.derpharmachemica.com

ISSN 0975-413X
CODEN (USA): PCHHAX

Der Pharma Chemica, 2016, 8(16):116-123
(http://derpharmachemica.com/archive.html)

Kinetic study of CO_2 capture over boric MFI zeolite

Bensafi Boumediéne*, Djafri Fatiha, Chouat Nadjat and Benchikh Imen

Laboratoire de chimie des matériaux, Département de Chimie, Université d'Oran 1 Ahmed BENBELLA, El M'naouer BP: 1524, Oran, Algérie

---

ABSTRACT

ZSM-5 zeolite has a great importance in hazardous substances adsorption and catalytic process. In this paper, a borosilicate ZSM-5zeolitewas carried out using N,N-dimethylaniline as a novel structure-directing agent. The synthetized material was characterized by X-ray diffraction, thermal analysis (TG/dTG), N_2 physical adsorption, and Fourier transform infrared spectroscopy. CO_2 adsorption was evaluated at different temperatures by a volumetric method, and both Langmuir and Freundlich adsorption models were applied. According to the experimental results, B-ZSM-5 zeolite has a favorable adsorption behavior at low temperatures. Different kinetic models were used to describe the adsorption of CO_2 over B-ZSM-5. A good agreement with experimental data was found for pseudo-n order.

Keywords: Zeolites, MFI, Organic template, CO_2adsorption, kinetic models.

INTRODUCTION

Zeolites are crystalline microporous aluminosilicates based on an infinitely extending three-dimensional four connected framework of AlO_4 and SiO_4tetrahedrals linked each other by an oxygen atom. Every SiO_4 tetrahedron in the framework bears a neutral charge, and every AlO_4 tetrahedron in the framework bears a net negative charge that is balanced by an extra-framework cation, which is usually an alkali or alkaline earth metal (1).Zeolites are classified according to the number of their opening pore,8 MR (Member of Rings) as small-pore, 10 MR as medium-pore, 12 MR as large-pore, and extra-large pore more than 12 MR systems(2).Their applications (ion exchange, adsorption, shape selectivity or catalytic activity) are essentially determined by their structures(3)and aluminum content in the framework(4).Zeolites include the natural type like chabazite (CHA), erionite (ERI) and clinoptilolite(HEU), and the synthetic types like A (LTA), X and Y (FAU), and ZSM-5 (MFI) (5).

As one of the most important zeolites in this field is ZSM-5 (Zeolite Socony Mobil with sequence number five), from structural type MFI. Its framework structure has bi-directional intersecting channels, one is straight and parallel to [010] direction with 5.1 x 5.7 Å and the other is sinusoidal in [100] direction with 5.4 x 5.6 Å, with an opening of 10-membered ring (6). It is widely used in adsorption (6)especially in catalytic process such as alkylation, aromatization, dehydration, and cracking(7-10). Borosilicate ZSM-5 (B-ZSM-5) zeolites are a class of high silica MFI type where aluminum atoms are substituted by boron atoms. This kind of synthesis was first conducted by Taramasso *et al.*(11). Since the physic-chemical properties behavior B-zeolite is different from Al-zeolite, it is expected that substitution of aluminum by boron would modify the acidic properties of zeolites(12).

It is well known that the template plays significant role in the synthesis of zeolites. The template can act as a structure directing agent, space filling and charge compensating species that is required for the successful synthesis of these materials (13,14). The structure and the size of the organic compound have a significant influence on the obtained zeolite(15). The ZSM-5 can be synthesized using different templates such as tetra-alkyl ammonium ions, amines and alcohols (16).

On the other hand, N,N-dimethylanilineis a tertiary amine of aniline derivatives. It is consisted of dimethylamino group coordinated to a phenyl group. N,N-dimethylaniline and their derivatives are used as a reagent for methyl furfural as a solvent for manufacturing of vanillinmichlers ketones (17), and can be used also as ligands in organometallic chemistry such as 4-formyl-N,N-dimethylaniline (18). It can be obtained from in-situ hydrogenation of nitrobenzene with hydrogen generated from methanol over Raney-Ni catalyst followed by alkylation. Recently, NNDMA is mostly produced from a two-step process involving the reduction of nitroarenes into anilines and the subsequent alkylation (19).N,N-dimethylaniline presents very interesting physical properties such a diameter of 0.622 Å and a volume of 76.7 $Å^3$(20), that is why it has been chosen as a voluminous molecule to obtain a zeolite with remarkable opening pores and high surface area.

Recently, a great attention has been given to the adsorption and separation of CO_2. Carbon dioxide is the main greenhouse gas, which causes a severe global warming. Its concentration in atmosphere is continuously increasing every year. Therefore, it is required to remove it from Natural and Flue gases for environmental and energy perception. Capture of CO_2 by adsorption has emerged as a potential technology due to low energy requirement and easy application (21). Industrially, the most used adsorbents are metal–organic frameworks, activated carbons, silica and alumina. In the last recent years, zeolites have been found suitable materials for this polluting gas elimination. Their structure, high surface area and physic-chemical properties such as hydrothermal and mechanical resistant made of them good adsorbents. Therefore, enormous efforts have been made by Scientifics to improve zeolites capture of CO_2 such as the work of Frantz *et al.*(6), where ZSM-5 have been prepared with high sodium content to improve its adsorptive properties. Chang Hun Lee *et al.*(22) tested the effect of pore structure on the CO_2 adsorption capacity using three types of organic templates.

In our knowledge, the N,N-dimethylaniline is one of the amines which have not been used as structure-directing agent in MFI structure synthesis. This study presents the first utilization of N,N-dimethylaniline as organic template in synthesis of borosilicate ZSM-5 zeolite and its application for CO_2 capture. In the literature, the Al-ZSM-5 zeolite has been proposed as potential candidate for CO_2adsorption process (23)due to its high adsorption capacity and simple regeneration. Here, we report the first work that carry out the utilization of the B-ZSM-5 in carbon dioxide adsorption.

MATERIALS AND METHODS

II.I Materials

The reagents used were: N,N-dimethylaniline (Sigma-aldrich, 99%) as organic template, porous silica gel powder (Fluka) as silicium source, sodium hydroxide pellets (Sigma-aldrich, 99.998%) as alkaline cation, boric acid (99.999%, Sigma-aldrich) as boron source, and demineralized water purified using Water Purification System Milli-Q (MERCK).

II.II Characterization

The pH value of the homogenous hydrogel was measured by inoLab pH 730 (WTW). The crystalline structure was determined by X-ray diffraction (Bruker AXS D8 ADVANCE diffractometer with a CuKα radiation source). Thermal analysis (TG/dTA) experiments were carried out by a TA Micrometrics 2050 TGA apparatus. The porosity occupied by the organic template was released by a calciner (Nabertherm). Textural properties of the material were measured by nitrogen physisorption (Micromeritics ASAP 2020). The FTIR spectra were taken in KBr pellets using Alpha-Bruker FTIR spectrophotometer.

II.IIIB-ZSM-5 synthesis

The hydrogel mixture was prepared by the following manner:
3 g of silica gel powder mixed with 0.8 g of sodium hydroxide solution, then 1.815 g N,N-dimethylaniline was added drop wise under stirring in a known volume of demineralized water. One hour later, 1.2 g of boric acid was added to the first mixture. The new mixture was stirred for 24h in room temperature till formation of homogenous hydrogel. After stirring, pH value was taken (pH = 11.68) and the hydrogel was allowed to aging. One hour later, the homogeneous mixture was transferred to a Teflon lined autoclave with a volume full capacity of 50 ml, then it was carried out in crystallization temperature of 423 K under autogenous pressure, for 6 days. After crystallization had been completed the autoclave was rapidly cooled and the recovered white solid was washed with deionized water, filtered off, and then dried at 373 K overnight. The dried zeolite sample wascalcined for 6h under atmospheric air at 773 K to eliminate the organic compound.

II.IV CO_2 adsorption

The carbon dioxide adsorption performance of the B-ZSM-5 sample was evaluated in the pressure range of 5 to 730 mmHg at different temperatures of 273 K, 288 K, and 298 K using CO_2gas with high purity (99.999 %). The adsorption measurement was carried out on Micromeritics ASAP 2020 apparatus. After every measurement, the

adsorbed CO_2molecules were desorbed by degassing gradually at 623 K for 4 hours to reach a vacuum. In order to investigate the adsorption behavior of the B-ZSM-5 zeolite, two isotherm models were proposed, Langmuir (Equation (1)) and Freundlich (Equation (2))(24):

$$q_e = \frac{q_m K_A P}{(1+K_A P)} \quad (1)$$

$$q_e = K_F P^{\frac{1}{n_F}} \quad (2)$$

WhereP: pressure of the gas [mmHg];q_e: solid phase adsorption quantity of carbon dioxide on zeolite at equilibrium [cm^3 STP/g]; K_A: Langmuir isotherm constant [1/ mmHg]; K_F: Freundlich isotherm constant; q_m: single layer CO_2 adsorption capacity [cm^3/g]; n_F: factor of heterogeneity.

RESULTS AND DISCUSSION

III.I XRD

X-ray diffraction (XRD) pattern of the synthesized B-ZSM-5 is illustrated on Figure 1. The reflection peaks are represented between the angles 2θ = 3° and 45°. According to the results, the main peaks are 2θ = 7.9, 8.8, 8.9, 23.2, 23.3, and 24°. Comparing to the collection of simulated XRD MFI-type zeolite (25), our synthesized B-ZSM-5 have the same peaks with high pure crystallinity and without any impurities.

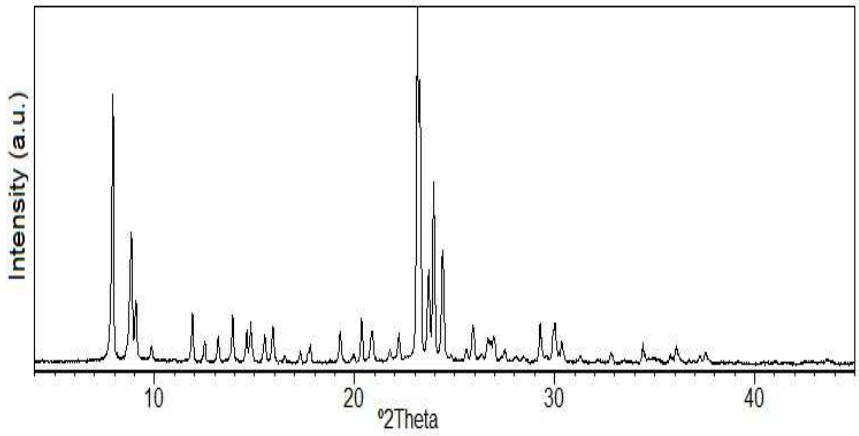

Figure1: XRD pattern of synthesized B-ZSM-5 zeolite

III.II Thermal analysis

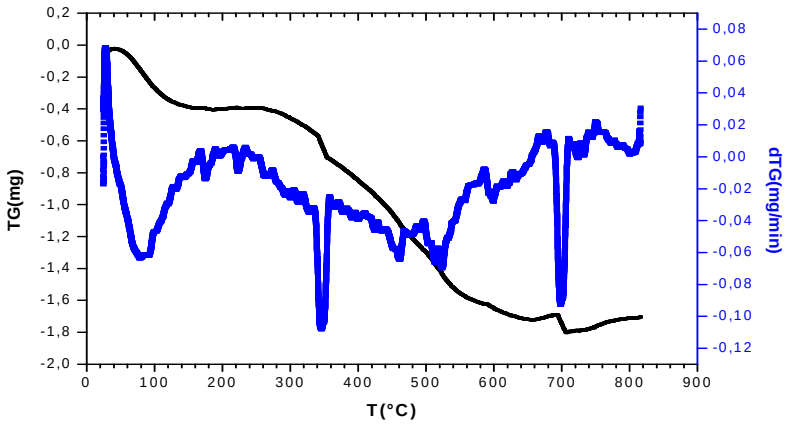

Figure 2: TG/dTG curves of synthesized B-ZSM-5 zeolite

The thermogravimetric analysis (TG/dTG) curves of the prepared mordenite are shown in Figure 2. The zeolite was heated from room temperature to 830 °C, at 10 °C/min, with 100 ml/min under air. The total mass lost was 1.8 mg. It represents both water and organic template losses. The first stage of weight loss was identified between 40 °C and 150 °C, that it is related to desorption of water molecules. In the first step, weakly bound water molecules are lost,

while some stronger ones are lost gradually. After this stage we see a stable level until 280 °C. In this range, there was any loss. The second stage was observed between 280 °C and 640 °C, it is related to mass loss caused by the thermodegradation of the organic template. At temperatures above 640°C, weight loss is associated with to thermofusion process of the zeolite.

III.III BET

Figure 3 shows N_2 adsorption-desorption isotherm of the sample B-ZSM-5. This isotherm provides valuable information on the textural properties of B-ZSM-5. For many microporous materials, in particular zeolites, the utilization of nitrogen at liquid temperature (77 K) is recommended. The specific surface area (S_{BET}) was evaluated by BET method using adsorption data in the range of a relative pressure from $p/p^0 = 0.05$ to $p/p^0 = 0.29$. The t-plot method was applied to determine the volume of micropores (V_{mic}). The adsorbed amount at relative pressure $p/p^0 = 0.98$ reflects the total adsorption capacity (V_{tot}). The void volume (V_{int}) account for the volume of interstices among zeolite particles. The values of determined textural properties are summarized in Table 1.

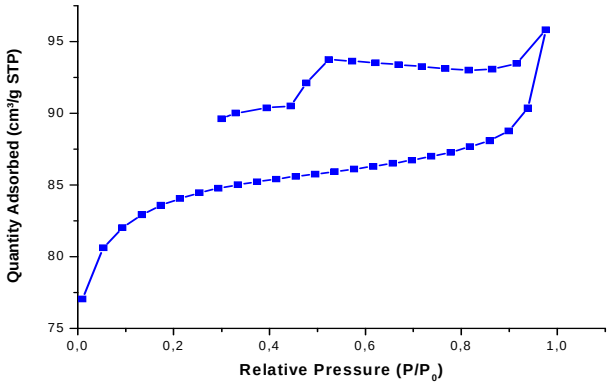

Figure 3: Nitrogen adsorption-desorption isotherm at 77 K of B-ZSM-5

Table 1:Textural properties of B-ZSM-5

S_{BET} (m^2/g)	S_{ext} (m^2/g)	S_{mic} (m^2/g)	V_{mic} (cm^3/g)	V_{voi} (cm^3/g)	V_{tot} (cm^3/g)
255.604	11.024	244.58	0.124	93.617	93.741

III.IV FTIR spectrum

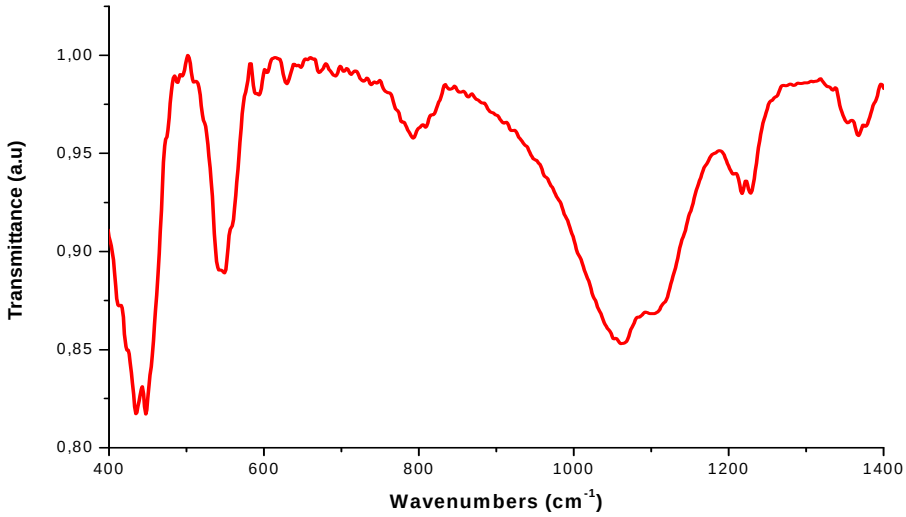

Figure 4: FTIR spectrum of synthesized B-ZSM-5 zeolite

FTIR spectrum of the synthesized sample is illustrated on Figure 4. Characteristics bands of ZSM-5 are shown in the spectrum. The bands at the regions of 1225 cm^{-1} and 1085 cm^{-1}, are respectively for external and internal asymmetrical stretching. For the external symmetrical stretching, characteristic band is around of 792 cm^{-1}. The five-member ring of pentasil structure of ZSM-5 zeolite is confirmed by the vibrational band at 549 cm^{-1}(26). Absorption bands at 1367 cm^{-1} and 629 cm^{-1} are attributed to stretching vibrations of the tetra-coordinated

framework boron, and Si-O-B symmetric bending (27), respectively. Finally, the band near to 450 cm^{-1} is attributed to the T-O bending vibration internal tetrahedral units of the SiO_4(28).

III.V CO_2 adsorption

As mentioned on Figure 5, the CO_2 adsorption over B-ZSM-5 zeolite at different temperatures 273 K, 288 K, and 298 K shows a regular variation of adsorbed amounts until upper pressure limit (730 mmHg) with an optimal adsorption capacity of 2.05 mmol/g. From curves, it is shown that adsorption is an inverse function of temperature, since; adsorption is reducing with increasing of temperature. It is important to mention that similar behavior of reduction in the adsorption of CO_2 at higher temperature has been observed in literature although with porous adsorbents materials and zeolites (29,30).

It is expected that borosilicate ZSM-5 zeolite has higher affinity with CO_2 molecules; it is due to the substitution of aluminum atoms by boron atoms into the ZSM-5 framework. It develops a low acidity in the zeolite lattice which can helps it in adsorption of CO_2 as acid gas. Interactions among the pores and the surface of B-ZSM-5 zeolite and the large quadruple moment of CO_2 have been pointing out as the factor which is responsible for the good uptake capacity found in this material.

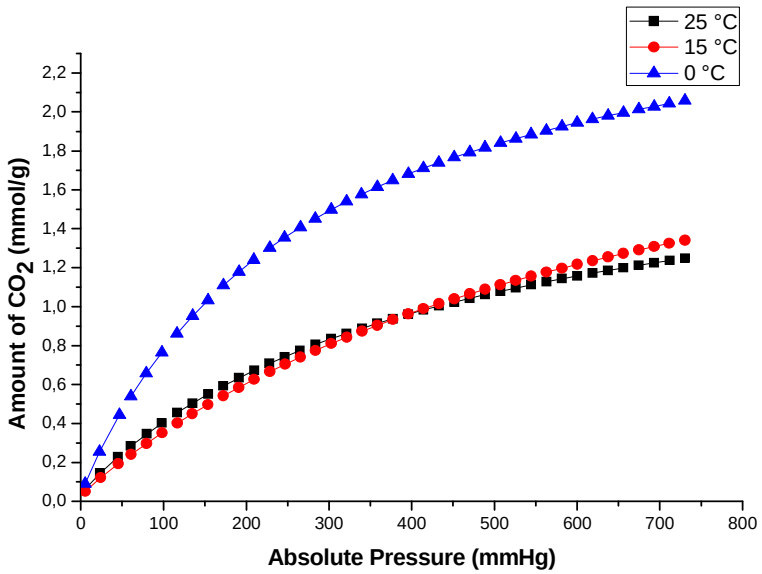

Figure5: Carbon dioxide adsorption at different temperatures

III.VI Langmuir and Freundlich models

The study of equilibrium is indispensable throughout all adsorption process. The experimental determination and modeling adsorption capacities of an adsorbent constitute the initial step to any adsorption process sizing. For this, two different isotherms models were tested, Langmuir and Freundlich.

The Langmuir model is based on simple assumptions (absence of interactions between adsorbed molecules, sites are energetically equivalent, and contain just one molecule adsorbed). Linearization of Langmuir equation (Equation (1)) is written as follows:

$$\frac{1}{q} = \frac{1}{q_m K_A} x \frac{1}{P} + \frac{1}{q_m} \qquad (3)$$

Freundlich model considers that there are different types of energy of different adsorption sites. The linearization of its equation (Equation (2)) is written as follows:

$$ln\, q = ln(K_F) + \frac{1}{n_F} ln(P) \qquad (4)$$

The Langmuir and Freundlich isotherm models fitting parameters, for the three different temperatures analyzed in this study and calculated respectively by Equation (3) and Equation (4), are summarized in Table 2.

Table 2:Langmuir and Freundlich constants at different temperatures

Temperature [K]	Langmuir			Freundlich		
	q_m [mmol/g]	K_A (10^{-4}) [1/mmHg]	R^2	K_F (10^{-4})	n_F	R^2
273	1.9193	89.66	0.9860	437.87	1.6526	0.9773
288	0.9567	100.24	0.9529	150.76	1.4492	0.9969
298	0.9327	136.66	0.9477	237.35	1.6289	0.9937

According to the results shown in Table 3,Freundlich model is more suitable than Langmuir for the two temperatures 288 K and 298 K. This is justified by the values of the regression coefficients which are high (R^2 = 0.9969, 0.9937 for Freundlich model, and R^2 = 0.9529, 0.9477 for Langmuir model at both temperatures 288 K and 298 K, respectively). However, at 273 K, the Langmuir model (R^2 = 0.9860) is more favorable than Freundlich model (R^2 = 0.9773), this is justified by their regression coefficients. So we conclude that, at temperatures 288 K and 298 K adsorptions takes place on various kinds of sites with different energies, while the adsorption at 273 K is carried out on the same sites energy and each site can sets a single molecule of CO_2.

III.VII Selection of the kinetic model

According to the literature, a large number of kinetic models [31] have been proposed to describe the adsorption process of different adsorbents. In this work, to choose a suitable kinetic model, variable models have been tested, such pseudo-first order (Equations (5)), pseudo-second order (Equations (6)), and pseudo-n order (Equations (7))(32,33,24).

- Pseudo-first order

$$\frac{dq_t}{dt} = k_f\,(q_e - q_t) \qquad (5)$$

After integration for limit conditions $q_t = 0$ at $t = 0$ and $q_t = q_e$ at $t = t$, Equation (5) can be written as follows (Equation (5')):

$$ln(q_e - q_t) = -k_f\,t + ln\,q_e \qquad (5')$$

- Pseudo-second order

$$\frac{dq_t}{dt} = k_s(q_e - q_t)^2 \qquad (6)$$

After integration for limit conditions, Equation (6) can be written as follows (Equation (6')):

$$\frac{t}{q_t} = \frac{1}{k_s \cdot q_e^2} + \frac{t}{q_e} \qquad (6')$$

- Pseudo-n order

$$\frac{dq_t}{(q_e - q_t)^n} = k_n\,dt \qquad (7)$$

After integration for limit conditions, Equation (7) can be written as follows (Equation (7')):

$$(q_e - q_t)^{1-n} = q_e^{1-n} + k_n(n-1)t \qquad (7')$$

Where q_e[mmol] and q_t [mmol] are, respectively, adsorption capacities at equilibrium and at time t [min], k_f pseudo-first order kinetic constant [min^{-1}], k_s pseudo-second order kinetic constant [min^{-1}], and k_n pseudo-n order kinetic constant [min^{-1}].

The kinetic model parameters for the CO_2 adsorption at 273 K which was consistent with the fitting results shown on Figure6are summarized in the Table 3. It can be observed that pseudo-n order had better results than other models. The utilization of the theoretical equation based on Avrami's model (34) leads to a value of n equal to 0.551 with minimal value of ($q_{e(exp)} - q_{e(theo)}$) and regression coefficient (R^2) superior to 0.99, thus attributed a good correlation between the theoretical model and experimental data. From these results, it can be concluded that the reaction is complex or multi pathway and the pseudo-n order model is the best for determining adsorption rate.

Table 3: Kinetic model parameters for CO_2 adsorption on B-ZSM-5 zeolite at 273 K

Pseudo order	Kinetic order	K	$q_{e(exp)}$	$q_{e(theo)}$	R^2
pseudo-first order	1	0.0666	2.0582	245.11	0.9133
pseudo-second order	2	0.0261	2.0582	0.3038	0.2702
pseudo-n order	0.551	0.0425	2.0582	1.5308	0.9975

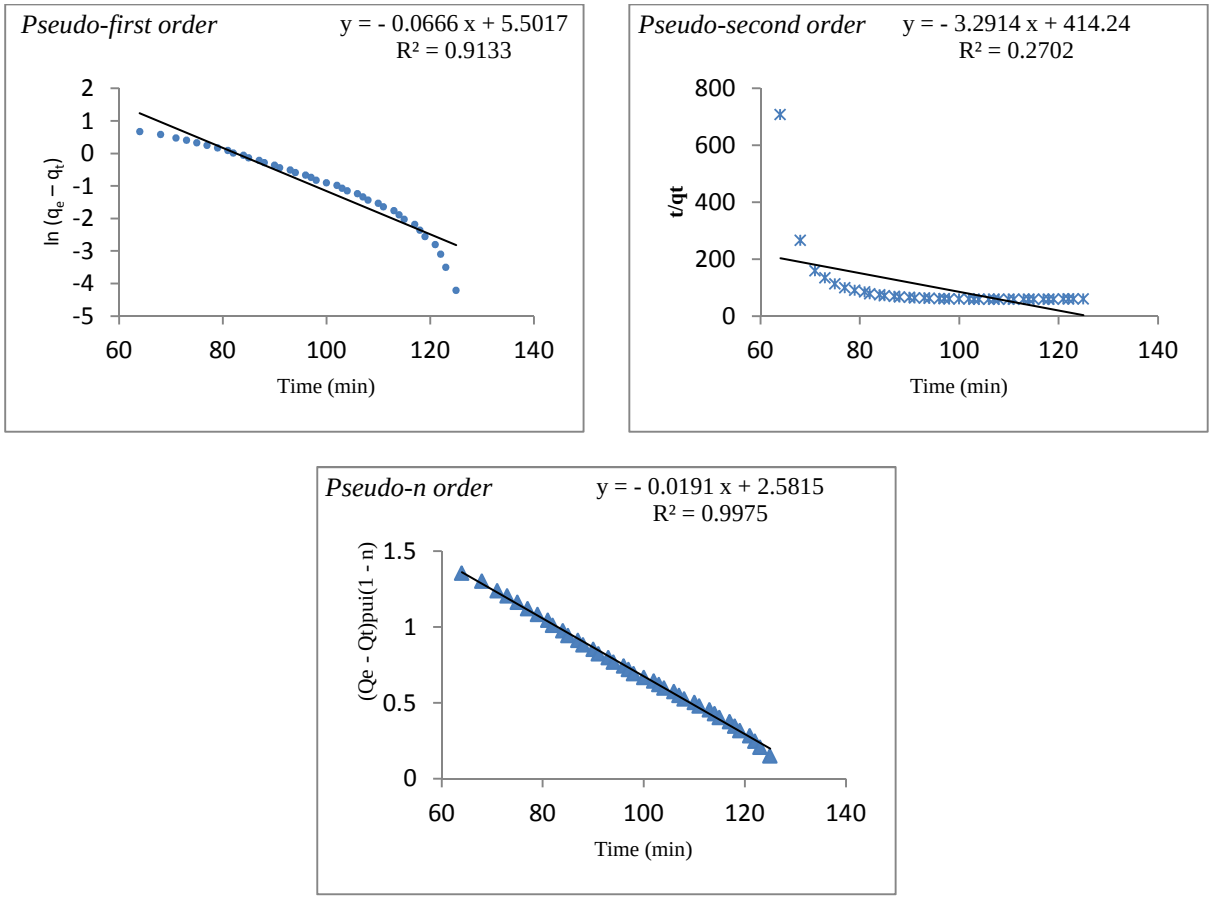

Figure 6:Pseudo-first second and n order kinetic models for CO_2 adsorption at 273 K

CONCLUSION

B-ZSM-5 was successfully synthesized using N,N-dimethylaniline as a novel organic template. The synthetized sample has a high specific surface area which makes of it a good adsorbent. The zeolite had favorable behavior during CO_2 adsorption especially at 273 K. This behavior was related to condensation of CO_2 in pores and external surface of the adsorbent. It has been found that Langmuir adsorption model is better than Freundlich adsorption model at 273 K to have the highest regression coefficient value, which explains that the adsorption has been done on the same sites energy and each site sets a single molecule of CO_2. The kinetic models have been applied to confirm the experimental results of CO_2 adsorption on B-ZSM-5. The pseudo-n order model (n = 0.551) validated all experimental results as its R^2 value is near of 1.

REFERENCES

[1] F.L. Deepak, A. Mayoral, R. Arenal, *Advanced Transmission Electron Microscopy: Applications to Nanomaterials*, Springer International Publishing, Switzerland, **2015**, p. 94.
[2] G. Busca, *Heterogeneous Catalytic Materials: Solid State Chemistry*, 1st Edition, Surface Chemistry and Catalytic Behaviour, Elsevier B.V., **2014**, p. 199.
[3] D. Xie, L.B. McCusker, C. Baerlocher, *Journal of the American Chemical Society*, **2011**, 133, 20604–20610.
[4] H. Van Bekkum, E.M. Flanigen, J.C. Jansen, *Introduction to zeolite science and practice*, Studies in Surface Science and Catalysis, Elsevier Science Publishers B.V., **1991**,58, p. 298.
[5] S. Kulprathipanja, *Zeolites in Industrial Separation and Catalysis*, WILEY-VCH Verlag GmbH & Co KGaA, Weinheim, **2010**, p. 35.

[6] T.S. Frantz, W.A. Ruiz, C.A. da Rosa, V.B. Mortola, *Microporous and Mesoporous Materials*, **2016**, 222, 209–217.
[7] H. Hu, Q. Zhang, J. Cen, X. Li, *Catalysis Communications*, **2014**, 57, 129–133.
[8] X. Zhang, L. Lin, T. Zhang, H. Liu, X. Zhang, *Chemical Engineering Journal*, **2016**, 284, 934–941.
[9] T.E. Tshabalala, M.S. Scurrell, *Catalysis Communications*, **2015**, 72, 49–52.
[10] X. Zhao, Lin Wei, S. Cheng, Y. Huang, Y. Yu, J. Julson, *Fuel Processing Technology*, **2015**, 139, 117–126.
[11] M. Abrishamkar, S.N. Azizi, H. Kazemian, *Chemistry of Metals and Alloys*,**2010**, 3, 12–17.
[12] R. Bandyopadhyay, Y. Kubota, N. Sugimoto, Y. Fukushima, Y. Sugi, *Microporous and Mesoporous Materials*,**1999**, 32, 81–91.
[13] T. Álvaro-Muñoz, C. Márquez-Álvarez, E. Sastre, *Catalysis Today*, **2012**, 179, 27–34.
[14] C. Yin, Y. Wei, F. Wang, Y. Chen, *Materials Letters*, **2013**, 98, 194–196.
[15] S. Sang, F. Chang, Z. Liu, C. He, Y. He, L. Xu, *Catalysis Today*, **2004**, 93-95, 729–734.
[16] U. Thubsuang, H. Ishida, S. Wongkasemjit, T. Chaisuwan, *Microporous and Mesoporous Materials*,**2012**, 156, 7–15.
[17] M. Gowrisankar, P. Venkateswarlu, K.S. Kumar, S. Sivarambabu, *Journal of Industrial and Engineering Chemistry*, **2014**, 20, 405–418.
[18] S. Packianathan, N. Raman, *Inorganic Chemistry Communications*, **2014**, 45, 55–60.
[19] K. Shimizu, K. Shimura, M. Nishimura, A. Satsuma, *ChemCatChem*, **2011**, 3, 1755–1758.
[20] Y. Marcus, *The Properties of Solvents*, Wiley Series in Solution Chemistry, volume 4, John Wiley & Sons Ltd, **1998**, p. 92.
[21] S. Sengupta, V. Amte, R. Dongara, A.K. Das, H. Bhunia, P.K. Bajpai, *Energy Fuels*, **2015**, 29, 287–297.
[22] C.H. Lee, D.H. Hyeon, H. Jung, W. Chung, D.H. Jo, D.K. Shin, S.H. Kim, *Journal of Industrial and Engineering Chemistry*, **2015**, 23, 251–256.
[23] S.K. Wirawan, D. Creaser, *Microporous and Mesoporous Materials*, **2006**, 91, 196–205.
[24] N. Chalal, H. Bouhali, H. Hamaizi, B. Lebeau, A. Bengueddach, *Microporous and Mesoporous Materials*, **2015**, 210, 32–38.
[25] M.M.J. Treacy, J.B. Higgins, *Collection of Simulated XRD Powder Patterns for Zeolites*, Fifth Revised Edition, Elsevier B.V., **2007**, p. 276.
[26] C. Li, Z. Wu,*Handbook of zeolite science and technology*, Microporous Materials Characterized by Vibrational Spectroscopies, chapter 11, **2003**.
[27] F. Thibault-Starzyk, *LES MATÉRIAUX MICRO ET MÉSOPOREUX: Caractérisation*, Groupe français des zéolithes, EDP Sciences, **2004**, p. 61.
[28] J. Jiang, C. Duanmu, Y. Yang, X. Gu, J. Chen, *Powder Technology*, **2014**, 251, 9–14.
[29] M.A. Sheikh, M.M. Hassan, K.F. Loughlin, *Gas Separation and Purification*, **1996**, 10, 161–168.
[30] S. Cavenati, C.A. Grande, A.E. Rodrigues, *Journal of Chemical and Engineering Data*,**2004**, 49, 1095–1101.
[31] G. Song, X. Zhu, R. Chen, Q. Liao, Y.D. Ding, L. Chen, *Chemical Engineering Journal*, **2016**, 283, 175–183.
[32] S.A.Wasay, M.J.Haron, A. Uchiumi, S. Tokunaga, *Water Research*,**1996**, 30, 1143–1148.
[33] Y.S. Ho, G. McKay, *Process Biochemistry*,**2003**, 383, 1047–1061.
[34] E.C.N. Lopes, F.S.C. dos Anjos, E.F.S. Vieira, A.R. Cestari, *Colloid Interface Science*, **2003**, 263, 542–547.